Capacity Bounds Analysis of 5G networks in different propagation environments

Aymen I. Zreikat
College of Engineering and Technology
American University of the Middle East
Kuwait
aymen.zreikat@aum.edu.kw

2023 IEEE 13th Annual Computing and Communication Workshop and Conference (CCWC) | 979-8-3503-3286-5/23/$31.00 ©2023 IEEE | DOI: 10.1109/CCWC57344.2023.10099143

***Abstract*— Due to a propagation phenomenon caused by reflection and diffraction in the radio channel of wireless networks, the transmitted signal is received by the receiver with multiple copies and different amplitudes, delays, and arrival angles. Compared to 4G, 5G networks provide massive applications with higher data rates, higher speed, low latency, and maximum capacity. Therefore, the strengths of the signal are a major issue to be considered for such systems. Not much research in the literature focused on deriving the capacity bounds in different propagation environments taking into account different types of environments. Therefore, it is crucial to study the capacity bounds of these systems in more realistic environments as the free space model does not take into account the environmental obstacles. Based on the above, the capacity bounds are derived due to cell interference and limited uplink power, and the performance of 5G networks in different propagation environments using the extended COST-231 Hata model, is studied in this paper. The capacity bounds are derived and the performance is evaluated in different environments for path loss evaluations and system capacity. The provided numerical results reveal the fact that system capacity and coverage are mainly affected by the type of environment and the service factor values. Consequently, the provided investigations and analysis provide key indicators for mobile operators to consider in the future planning of 5G networks.**

Keywords—Capacity Bounds, 5G Networks, Propagation environments, COST-231 Hata model, Performance Evaluation.

I. INTRODUCTION

5G networks stand for the fifth generation cellular networks where the service area is divided into small hexagonal shapes of small geographical areas called cells. As mentioned in [1], there are yet numerous demands that need to be managed by research centers before the final employment of 5G takes place.

The network infrastructure of 5G networks is based on the Millimeter wave (mm-Wave) band [2-3] that can be utilized in broadband access of a wide range of services with low latency, higher speed, and higher data rate. Besides, the Antennas of mm-Wave bands are very suitable for many Internet of things (IoT) applications that require some special and small devices. Under these circumstances, capacity is expected to be maximized. On the other hand, propagation phenomena hurt signal strength, and sometimes this status requires the use of small cell sizes for Wi-Fi and cellular network structure. Therefore, the performance and analysis of such systems should be conducted under real-life scenarios taking into consideration the propagation phenomena in different environments such as dens-urban, urban, suburban, and rural.

In mobile communications, the transmitted signal should arrive at the receiver with the required strength to satisfy the network QoS conditions as well as an acceptable coverage over the service area. Usually, in real-life environments with multipath propagation phenomena that cause diffraction, scattering, or reflections, the required strength at the receiver is not achieved. Therefore, performance evaluation and capacity bounds analysis of such systems should consider the path loss effect in different propagation environments.

The original Hata model is suggested in [4] which was based on the empirical Okumura Hata models [5]. The path loss propagation models provided by Okumura Hata have limited path lengths and frequency ranges. Because of this, some extended models are developed in the literature such as the extended COST-231 Hata model to incorporate greater path lengths and higher frequency ranges to handle the requirements of the new technology.

The contribution of this research work is as follows. What is significant about this research work is that the capacity bounds are derived in different propagation environments concerning two important factors that affect the performance, namely, the interference and the limited uplink transmission power. Therefore, the provided analysis, discussion, and the obtained numerical results will offer a significant key indicator for mobile operators to be considered in the future planning of 5G networks.

The remainder of this research work is structured as follows. Related work comes in Section II. An overview of the extended Hata Model is in Section III. Capacity bounds analysis is in Section IV. The simulation results and discussion are in Section V. Finally, in Section V1 the conclusions and future work are given, followed by the list of references.

II. RELATED WORK

Due to the recent shift of the technology from 4G to 5G systems, mobile operators are facing tremendous challenges as people are moving from traditional applications to a new design of the network, which supports diverse applications that connect machines, objects, and devices virtually with multi-gigabit speed, negligible latency, and maximum spectrum efficiency. To overcome the above challenges, it is crucial to study the capacity bounds of these systems in more realistic environments to reflect the end-user experience more realistically. The capacity bounds are studied and analyzed in the literature from different authors' views, and perspectives.

In some previous literature studies [6], the authors considered the Shannon capacity formula to derive the system

capacity. Long-term evolution (LTE) was the case study in this work where authors predicted LTE spectral efficiency in micro and macro environments. Through the generated results, the authors claim a perfect match between the predicted and the simulation values. The capacity bounds are derived in [7] with spectral constraints and quantization techniques. The authors came up with a conclusion that although using low quantization resolution has a minimum effect on 5G systems' achievable rates, satisfying out-of-band limits is a challenge for the future of 5G systems. The authors in [8] proposed QoS provisioning, which has a statistically limited delay parameter for multimedia mobile wireless networks such as 5G, by using a finite block length coding. Capacity formulation of such systems is taken into consideration by delay-bounded QoS constraints. The authors validate the system performance results by simulation results.

In the latest literature, [9-15] authors have studied the capacity bound based on different factors and views. In [9], the authors derived the error probability and capacity bounds based on the special modulation symbols of the vertical bell labs space-time system. The authors derived the average bit error probability upper bound and developed an efficient error correction mechanism. The authors claimed that the proposed detection is very convenient for the spatial modulation scheme, which is multiple input multiple outputs (MIMO) modulation detectors compared to a compressive sampling matching pursuit detector. Efficient Capacity analysis and transceiver design are derived in [10] to overcome the two main problems facing rail train carriages; namely, the time-varying of channel parameters and the loss of the signal. Unlike the current traditional techniques to solve these problems such as relaying or beamforming, the authors claim that the suggested techniques outperform the current techniques. Lower and upper bounds of capacity are derived with a suggestion of transceiver design and simulation results confirm that the anticipated technique will be very useful for future channel estimations. The authors claimed in [11] that, unlike other work in the literature, a device-to-device communication model is proposed assuming a nun-ideal transceiver with interference and a lack of channel state information. The closed form of the upper and lower capacity bounds are derived using saddle point approximations. Capacity results are validated against Monte Carlo simulation and it is shown by the numerical results that the mmWave communication can resist the transceiver noise even under higher values of signal to Noise ratio (SNR). Given the positive effect of the multiple input multiple outputs (MIMO) relay model on the coverage and capacity of the next-generation wireless networks, the authors in [12] have examined the influence of the remaining hardware impairments on the ergodic capacity of dual-hop (DH) amplify and forward (AF) MIMO relay systems. In addition to deriving the upper and lower limits of capacity, the authors studied the effect of low values of SNR on system capacity via simulation. Authors claim by simulation results that the capacity goes into saturation with degradation of the transceiver when there are multiple antennas and different values of SNR. In [13], the upper bounds of the capacity are derived for the large intelligent surface (LIS) antenna concept. A greedy scheduling scheme is proposed and via Monte Carlo simulation, the authors claim that maximum capacity can be gained in areas with a large number of LIS. A new path loss model was suggested in [14] for urban areas considering new parameters such as window size, humidity, and temperature. The authors claimed that the proposed model improves the estimation of the path loss by 10% compared to other models in the literature.

III. THE EXTENDED COST-231 HATA MODEL

Unlike COST-231 Hata, the extended version of the empirical model suggests a general path propagation equation to substitute the signal strength due to the path loss and to cover a higher range of frequencies. The general free-space model [15] encompasses two terms; a logarithm part based on the distance and another logarithm part based on the frequency as shown below:

$$PL_E(d) = PL_0(d) = 32.44 + 20 \cdot log(f) + 20 \cdot log(d) \quad (1)$$

Where E is zero for a free space model as per the assumed codes given in Table 1 for each type of environment, E.

However, the propagation loss equations are derived in this study for different realistic environments such as dense urban, urban, suburban, and rural based on the provided propagation equation given in [16] as follows:

$$PL_E = 46.3 + 33.9 \cdot log(f) - 13.82 \cdot log(h_b) - a(h_m) + (44.9 - 6.55 \cdot log(h_b)) \cdot log(d) + CF_E \quad (2)$$

Definition. We introduce CF_E as a correction factor for each environment type E. PL_E is the path loss for environment type E in dB as assumed in Table 1. f is the frequency in MHz. h_b is the height of the base station or transmitter in meters, m. h_m is the height of the mobile or receiver in meters. d is the distance between transmitter and receiver in kilometers, Km. $a(h_m)$ is the correction factor for the mobile antenna.

Note that in (2), the propagation loss equation will be different in each environment concerning two parameters; namely $a(h_m)$ and CF_E.

Therefore, the propagation loss equations [17] are derived using (2) to obtain:

1. The propagation model for the urban environment is as follows:

$$PL_1 = 46.3 + 33.9 \cdot log(f) - 13.82 \cdot log(h_b) - a(h_m) + (44.9 - 6.55 \cdot log(h_b)) \cdot log\ (d) \quad (3)$$

Where,

TABLE 1: CODES ASSUMED FOR EACH ENVIRONMENT

Environment Type, E	Code
Free space	0
Urban	1
Suburban	2
Dense urban	3
Rural	4

$a(h_m) = (1.1 \cdot log(f) - 0.7) \cdot (h_m) - (1.56 \cdot log(f) - 0.8)dB$

2. The propagation model for the suburban environment is as follows:

$$PL_2 = PL_1 - 2 \cdot \left(log\frac{f}{28}\right)^2 - 5.4 \quad (4)$$

3. The propagation model for the dense urban environment is as follows:

$$PL_3 = 46.3 + 33.9 \cdot log(f) - 13.82 \cdot log(h_b) - a(h_m) + (44.9 - 6.55 \cdot log(h_b)) \cdot log(d) + 3 \quad (5)$$

Where

$$a(h_m) = 3.2 \cdot (log(11.75 \cdot h_m)^2 - 4.97dB$$

4. The propagation model for the rural environment is as follows:

$$PL_4 = PL_1 - 4.78 \cdot (log(f))^2 + 18.33 \cdot log(f) - 40.94 \quad (6)$$

IV. Capacity Bounds Analysis

A. Capacity bounds due to the interference

In wireless communications, it is known that each active user in the cell provides interference to other users. As the number of active users increases, user *i* should increase power to cope with node requirements. We consider a system with a single service case. Therefore, it is assumed that all users are transmitting a signal with the same spreading factor, SF_i, and hence, the required SNR_i is achieved to all users (S_i=SF_i/SNR_i=S). Furthermore, the non-orthogonality factor, ε_{ij} will be equal for all code combinations (ε_{ij}=ε). Following the derivation of P_R in [17] and assuming that all users in the cell are using the same radio service, with n users interfering with each other in the cell, a thermal noise; N_0 is created in the cell and derived as follows:

$$N_0 = P_R \cdot \left(S - (n-1) \cdot \frac{V \cdot \varepsilon}{F}\right) \quad (7)$$

Because of the linear relationship between the received power of user *i*, PR_i, and the interference caused by other users in the cell, the system will not be able to improve the signal-to-noise ratio (*SNR*) when the number of active users, n_{max} reaches a specific limit. Therefore, from (7), we get

$$n_{max} < \frac{S \cdot F}{\varepsilon . V} + 1 \quad (8)$$

Definition. n_{max} is the maximum number of active users in the cell, ε is the non-orthogonality factor of the user's signals, S is the service factor (S = SF/SNR), and SF is the spreading factor representing the number of chips per data symbol. V is the activity factor for any type of user service and F is the inter-cell interference factor.

B. Capacity Bounds Due To The Limited Uplink Transmission Power

The maximum transmitted power; P_{Smax} of the user equipment (UE) depends on the distance, d between the UE and Node B. Therefore, UE may not be able to achieve the desired received power, P_R at Node B, due to the path loss. Because of this fact, it is very well known the following [6]:

$$P_R = P_{Smax} \cdot PL_E(d_{max}) \quad (9)$$

Definition. P_R is the power received at Node B, P_{Smax} is the maximum power sent by the UE, $PL_E(d_{max})$ is the path that depends on the distance between the UE and Node B and the parameter E is the code to be used for the type of environment (free space, urban, dense-urban, suburban, and rural).

However, for the real environment, the power budget will not be perfect. Therefore, the power control error (P_{err}) should be considered in the path loss as a substitution for the difference between the real and the estimated path loss due to fading phenomena. Consequently, (9) should be written as:

$$P_R = P_{Smax} \cdot PL_E(d_{max}) \cdot P_{err} \quad (10)$$

Then,

$$PL_E(d_{max}) = \frac{P_R}{P_{Smax} \cdot P_{err}} \quad (11)$$

By substituting the value of P_R from (7) into (11), we get:

$$PL_E(d_{max}) = \frac{N_0}{\left(S-(n-1)\cdot\frac{V\cdot\varepsilon}{F}\right)\cdot P_{Smax}\cdot P_{err}} \quad (12)$$

Recall [6] and [7], the path loss for free space propagation is formulated as

$$\frac{P_R}{P_{Smax}} = \left(\frac{\lambda}{4\cdot\pi\cdot d_{max}}\right)^2 \cdot g_b \cdot g_m = PL_E(d_{max}) \quad (13)$$

Substitute $PL_E(d_{max})$ value from (12) into (13) and since P_R is dependent on the number of active users in a single cell case, the antenna gains g_b, g_m and are P_{err} are all assumed to be 1. We get

$$\left(\frac{\lambda}{4\cdot\pi\cdot d_{max}}\right)^2 = \frac{N_0}{\left(S-(n-1)\cdot\frac{V\cdot\varepsilon}{F}\right)\cdot P_{Smax}} \quad (14)$$

Definition. λ is the wavelength $\lambda = c/f$ (c is the speed of light and f is the frequency), and d_{max} is the maximum distance between UE and Node B.

Assuming a single service case, then the received power, P_R is completely dependent on the number of active users in the cell, n. According to cell breathing phenomena [5][8] shown in Fig. 1, when the load of the cell increases, the cell effective coverage shrinks as this new user brings more interference to other users. Therefore, the adjacent cells will be the best candidate for users who are at the cell borders.

From (14) and based on the derivation in [1], the new formula for d_{max} as a function of n can be formulated as follows:

$$d_{max}(n) = \frac{\lambda}{4\cdot\pi} \cdot \sqrt{\frac{P_{Smax}\cdot PL_E(d)}{N_0} \cdot \left(S - (n-1)\cdot\frac{\varepsilon\cdot V}{F}\right)} \quad (15)$$

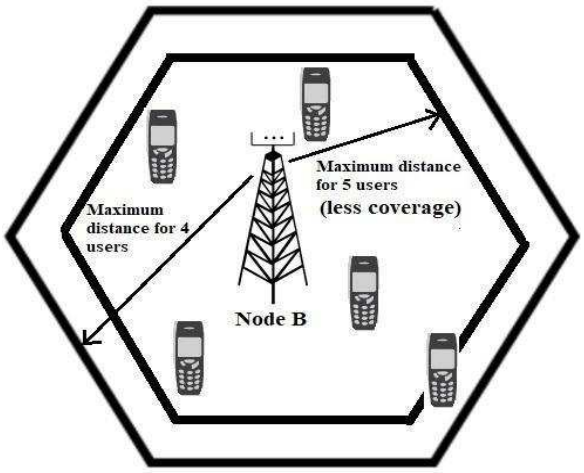

Fig. 1: Cell breathing phenomenon

C. Single Service Capacity Bounds

Mobile operators should take into account the coverage of a given cell, as the maximum number of active users in the cell changes dynamically. Therefore, in cell planning, it is important to consider the users who are active based on cell coverage and on the provided radio link service.

Because of this, from (14) the maximum number of active users, n_{max} can be derived as follows:

(14) can be rewritten as,

$$\left[S - \left(\frac{(4\cdot\pi\cdot d_{max})^2\cdot N_0}{P_{Smax}\cdot\lambda^2}\right)\right]\cdot\frac{F}{V\cdot\varepsilon} = n_{max} - 1 \quad (16)$$

Therefore,

$$n_{max} = \left[S - \left(\frac{(4\cdot\pi\cdot d_{max})^2\cdot N_0}{P_{Smax}\cdot\lambda^2}\right)\right]\cdot\frac{F}{V\cdot\varepsilon} + 1 \quad (17)$$

Additionally, assuming that the cell covers an ideal circle with the cell radius, r then (17) can be rewritten to represent the maximum number of active users in the cell as follows

$$n_{max} = \left[S - \left(\frac{(4\cdot\pi\cdot r)^2\cdot N_0}{P_{Smax}\cdot\lambda^2}\right)\right]\cdot\frac{F}{V\cdot\varepsilon} + 1 \quad (18)$$

V. Simulation Results with Discussions

Using MATLAB simulation, the numerical results are prepared according to the parameters listed in Table 2. Seven figures are shown in this analysis. Fig. 2 shows the path loss in different propagation environments based on the derived formulae for each environment. It can be noticed that low loss values are achieved when a free space environment is assumed, as there is a clear line of sight between the transmitter and the receiver without obstacles. It can also be noticed that losses are higher in the rural environment than in open space, especially when the distance is more than 5 km since in rural areas there is no clear line of sight between transmitter and receiver compared to the free space model. Furthermore, unlike free space, rural areas can contain buildings and airports, but with fewer people compared to other environments.

Dense urban areas have the highest path losses since it contains a high density of population, and crowded buildings, and therefore, they usually suffer from signal radiation. The maximum distance from Node B is shown in Fig. 3 for different service factor values. The lower the service factor the higher the data rate but the coverage area will be minimized. For example, it can be noticed from Fig. 3 that when S is 8, the coverage is only within a range of 6 km away from Node B where around 40 users are covered with this service. On the other hand, when S is 128 then more than 500 users can be covered within a round distance of 22 km. In Fig. 4, the relationship between the cell capacity and the cell radius is shown but also under the effect of different service factors. It can be noticed that at a higher value of S (S=128), the capacity of the cell is maximized as a large number of users can be covered as long as the cell radius is increased. This figure shows the positive relationship between the value of S and the cell radius from one side and the positive effect of this relationship on the total capacity of the cell. Similar behavior can be seen in the figures (Fig. 5-Fig. 7) but this time the aim is to demonstrate the environmental effect on the cell capacity. Again, higher values of S lead to an increase in system coverage and capacity. As shown in Fig. 5, when S = 128 and the environment is a free space, 250 users are covered with the available service considering that the data rate will be reduced for each user as all users are sharing the resources at the same time. Similar behavior can be seen in Fig. 6 and Fig. 7. When S goes down, the number of active users decreases dramatically. Because of this, users will get a better data rate. The last figure in this analysis is Fig. 8 where the relationship between the distance from Node B and the capacity is shown for the three major types of environments, namely; dense urban, urban, and suburban. For example, it can be noticed that 150 users can be covered with service at around 1.5 km distance in suburban areas, where people are located in areas with less population compared to urban and dense urban areas. On the contrary, the same number of users is achieved at about 0.9 *Km* from Node B in urban areas and about 0.5 *km* in dense urban areas where population density is high. Furthermore, Fig. 8 illustrates the phenomenon of cellular breathing, as it shows that coverage decreases when the number of users in the cell increases, as the new user interferes with other users. This is a key indicator to be considered by mobile operators in cell planning of future 5G networks.

TABLE 2. SIMULATION PARAMETERS

Parameter	Value
Number of codes, N	64
Frequency, f	20 *GHz*
Height of the mobile, h_m	1.5 *m*
Height of the base station, h_b	50 *m*
Service Factor, *S(SF/SINR)*	16, 32, 64, 128
Cell radius, r	0-20 *Km*
Spreading factor, *SF*	32, 64, 128, 256 *chips/symbol*
Maximum transmission power, *Psmax*	120*W*
Thermal Noise, N_0	-103 *dBm*
Signal to Interference Noise Ratio, *SINR*	2 *dB*
Interference factor, ε	0.50
Wave length, λ	0.15 *m*

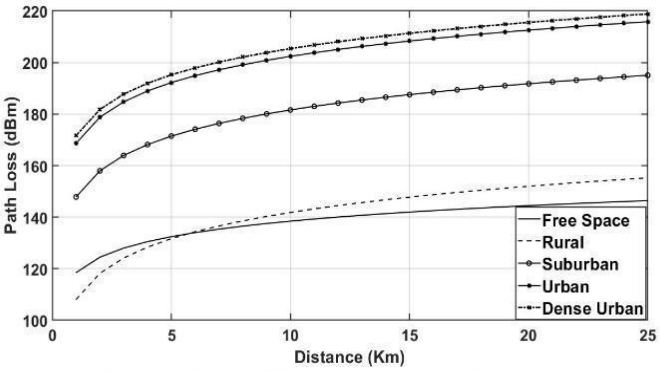

Fig. 2: Path loss in different propagation environments

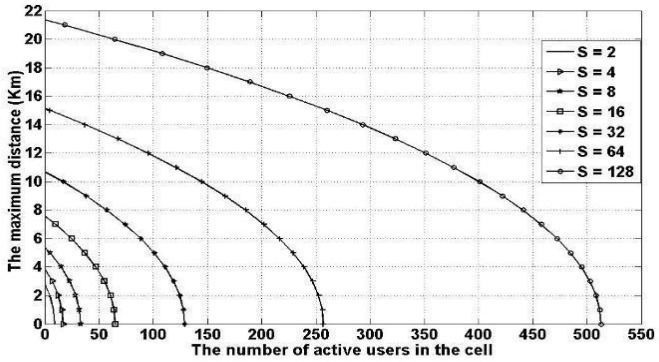

Fig. 3: The maximum distance (coverage area vs. capacity)

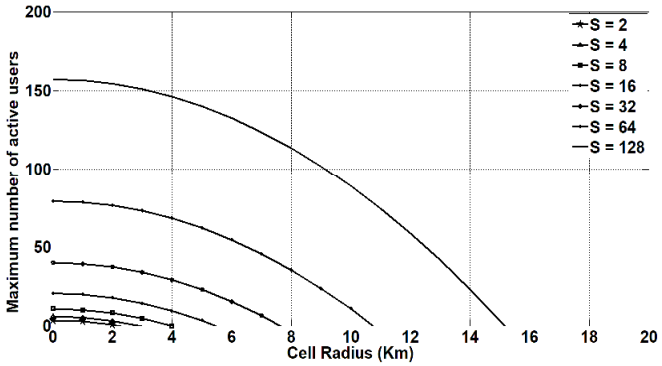

Fig. 4: Cell capacity for different service factors, *S* values

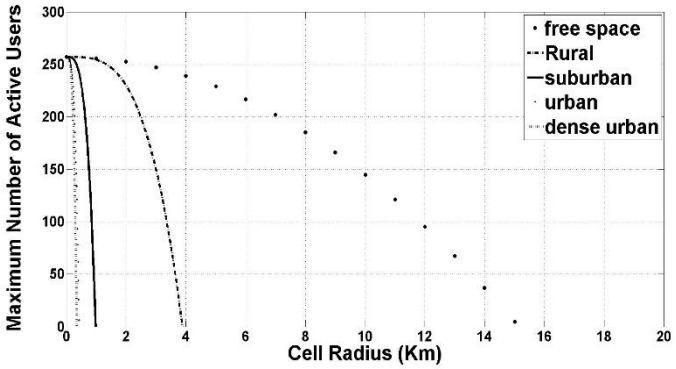

Fig. 5: Cell capacity in different propagation environments, S =128

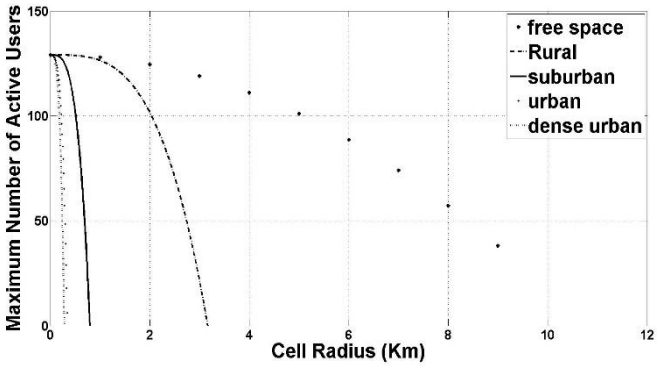

Fig. 6: Cell capacity in different propagation environments, S = 64

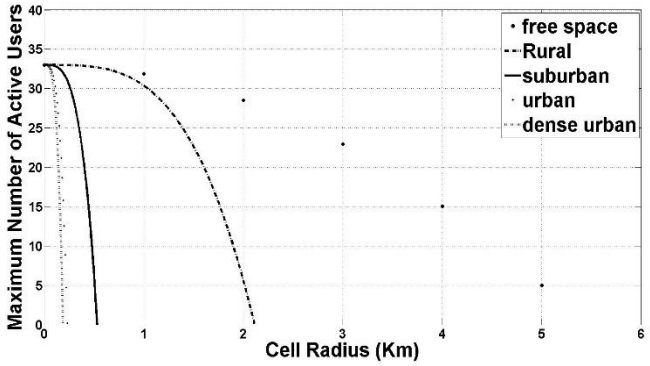

Fig. 7: Cell capacity in different propagation environments, S = 16

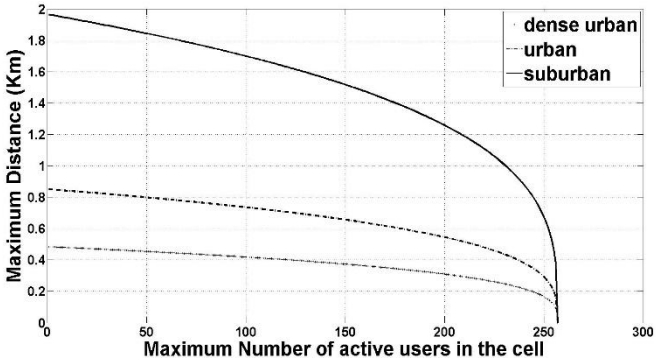

Fig. 8: Maximum distance in different propagation environments

VI. CONCLUSION AND FUTURE WORK

In wireless networks, the transmitted signal is received by the receiver with multiple copies and different amplitudes, delays, and arrival angles due to the propagation phenomenon caused by reflection and diffraction. Compared to 4G, 5G networks provide massive applications with higher data rates, higher speeds, low latency, and maximum capacity. Besides, the strengths of the signal are a major issue to be considered for such systems. Furthermore, it is crucial to study the capacity bounds of these systems in more realistic environments as the free space model does not take into account the environmental obstacles. In this research, the capacity bounds in different propagation environments are derived considering cell interference and limited uplink power. It is also shown that the system capacity and coverage are mainly affected by the type of environment and the service factor parameter. The provided investigations and analysis provide key indicators for mobile operators to consider in the future planning of 5G networks.

Please note that this study only focuses on a single service case. For multi-service cases, the capacity bounds need to be derived take into account additional parameters such as different radio link services, k that leads to different service factors, S_k. Therefore, the capacity limits in different propagation environments in multi-service cases can be considered as a possible extension of the current work to be carried out in the future. Furthermore, the analysis performed in this research can be extended to a multi-cell scenario where

seamless 5G handover between the original cell and neighboring cells can be considered. Finally, a comparison with similar work having the same scenario, if found, would be very useful to be conducted in future research work.

REFERENCES

[1] A. I. Zreikat, "Load balancing call admission control algorithm (CACA) based on soft-handover in 5G Networks," 2022 IEEE 12th Annual Computing and Communication Workshop and Conference (CCWC2022), 2022, pp. 0863-0869.

[2] J. Chen, W. Lin, P. Yan, J. Xu, D. Hou, and W. Hong, "Design of mm-Wave transmitter and receiver for 5G," 2017 10th Global Symposium on Millimeter-Waves, 2017, pp. 92-93.

[3] F. K. Banaseka and S. Dotse, "New deployments and Research challenges for 5G wireless systems and networks", International Journal of Current Research, Vol. 9, Issue, 02, February 2017, pp. 46626-46631.

[4] M. Hata, "Empirical formula for propagation loss in land mobile radio services," in IEEE Transactions on Vehicular Technology, Vol. 29, No. 3, pp. 317-325, Aug. 1980.

[5] N. S. Nkordeh, A.A.A Atayero, F.E Idachaba, O.O Oni. "LTE Network Planning using the Hata-Okumura and the COST-231 Hata Path loss Models, " Proceedings of the World Congress on Engineering 2014, Vol I, WCE 2014, July 2 - 4, 2014, London, U.K.

[6] P. Mogensen et al., "LTE Capacity Compared to the Shannon Bound," 2007 IEEE 65th Vehicular Technology Conference - VTC2007-Spring, 2007, pp. 1234-1238, DOI: 10.1109/VETECS.2007.260.

[7] S. Dutta, A. Khalili, E. Erkip and S. Rangan, "Capacity Bounds for Communication Systems with Quantization and Spectral Constraints," 2020 IEEE International Symposium on Information Theory (ISIT), 2020, pp. 2038-2043, DOI: 10.1109/ISIT44484.2020.9174260.

[8] X. Zhang, J. Wang, and H. V. Poor, "Statistical Delay-Bounded QoS Provisioning Over 5G Multimedia Mobile Wireless Networks in the Finite Blocklength Regime," ICC 2019 - 2019 IEEE International Conference on Communications (ICC), 2019, pp. 1-6, DOI: 10.1109/ICC.2019.8761713.

[9] L. Xiao, P. Xiao, Z. Liu, W. Yu, H. Haas, and L. Hanzo, "A Compressive Sensing Assisted Massive SM-VBLAST System: Error Probability and Capacity Analysis," in IEEE Transactions on Wireless Communications, vol. 19, no. 3, pp. 1990-2005, March 2020, DOI: 10.1109/TWC.2019.2960505.

[10] W. Zhao, G. Wang, B. Ai, J. Li, and C. Tellambura, "Backscatter Aided Wireless Communications on High-Speed Rails: Capacity Analysis and Transceiver Design," in IEEE Journal on Selected Areas in Communications, vol. 38, no. 12, pp. 2864-2874, Dec. 2020, DOI: 10.1109/JSAC.2020.3005494.

[11] L. Tlebaldiyeva, B. Maham and T. A. Tsiftsis, "Capacity Analysis of Device-to-Device mmWave Networks Under Transceiver Distortion Noise and Imperfect CSI," in IEEE Transactions on Vehicular Technology, vol. 69, no. 5, pp. 5707-5712, May 2020, DOI: 10.1109/TVT.2020.2983417.

[12] A. K. Papazafeiropoulos, S. K. Sharma, S. Chatzinotas and B. Ottersten, "Ergodic Capacity Analysis of AF DH MIMO Relay Systems With Residual Transceiver Hardware Impairments: Conventional and Large System Limits," in IEEE Transactions on Vehicular Technology, vol. 66, no. 8, pp. 7010-7025, Aug. 2017, DOI: 10.1109/TVT.2017.2668460.

[13] F. Cao, Y. Han, Q. Liu, C. -K. Wen and S. Jin, "Capacity Analysis and Scheduling for Distributed LIS-aided Large-Scale Antenna Systems," 2019 IEEE/CIC International Conference on Communications in China (ICCC), 2019, pp. 659-664, DOI: 10.1109/ICCChina.2019.8855854.

[14] Z. Nossire, N. Gupta, L. Almazaydeh, X. Xiong, "New Empirical Path Loss Model for 28 GHz and 38 GHz Millimeter Wave in Indoor Urban under Various Conditions,", Appl. Sci. 2018, Vol. 8, No. 11: 2122. https://doi.org/10.3390/app8112122

[15] J. D. Parsons: Mobile Radio Propagation Channel, J. Wiley & Sons, Second Edition, pp. [16-17, 75-77,116-118], 2000.

[16] COST231 (1999): Digital Mobile Radio: Towards Future Generation Systems", Final Report, EUR18957, Chapter 4, 1999.

[17] A. I. Zreikat, "Radio Resource Management and Modeling for Wireless Mobile Networks: Enhancement of Call Admission Control Algorithms (CACAs) and Capacity Bounds in UMTS/GSM Networks," published in LAMBERT Academic Publishing, Germany, 216 pages. (ISBN-10: 3846534994, ISBN-13: 978-3846534991).